Afyon Kocatepe Üniversitesi Fen ve Mühendislik Bilimleri Dergisi
Afyon Kocatepe University – Journal of Science and Engineering
https://dergipark.org.tr/tr/pub/akufemubid

Araştırma Makalesi / Research Article
DOI: https://doi.org/10.35414/akufemubid.1425085
AKÜ FEMÜBİD 24 (2024) 045703 (940-946)
AKU J. Sci. Eng. 24 (2024) 045703 (940-946)

Air Atmosphere Sintering and Characterization of Dense Si_3N_4 Ceramics

*Makale Bilgisi / Article Info
Alındı/Received: 25.01.2024
Kabul/Accepted: 09.06.2024
Yayımlandı/Published: 20.08.2024

Yoğun Si_3N_4 Seramiklerinin Hava Atmosferinde Sinterlenmesi ve Karakterizasyonu

Gülsüm TOPATEŞ

Ankara Yıldırım Beyazıt University, Department of Metallurgical and Materials Engineering, Ankara, Türkiye

Abstract

Air atmosphere sintering was successfully applied for Si_3N_4 ceramics at 1550°C by using a double crucible setup. Low weight loss values showed that this setup eliminated the risk of oxidation. Both sintering time and type of starting Si_3N_4 powder affected the final properties of samples. Sintered densities reached 3.04 and 2.86 g/cm^3 at 3 h for Ube and SicoNide sources, respectively. Around 10 wt. % of β-Si_3N_4 is existing in SicoNide powder according to XRD analysis. FTIR study also proved the presence of this phase. This directly retards densification owing to the lower reactivity of β-phase compare to α. The major phase formed was β-Si_3N_4 with a minor amount of α-Si_3N_4 and Si_2N_2O. Large β-grains were also observed by SEM images from both samples sintered at 3 h. Hardness, fracture toughness, and dielectric constant values were 12.5 GPa, 5.8 MPa.m$^{-1/2,}$ and 7.84, respectively. These results showed that air sintering may be a suitable alternative for the low-cost production of Si_3N_4 ceramics.

Keywords: *Si_3N_4; Air sintering; Starting powder; Sintering time; Densification.*

Öz

Si_3N_4 seramikleri, çift pota düzeneği kullanılarak 1550°C'de hava atmosferi altında başarılı bir şekilde sinterlenmiştir. Düşük ağırlık kayıpları, düzeneğin oksidasyon riskini ortadan kaldırdığını göstermiştir. Sinterleme süresi ve Si_3N_4 başlangıç toz türü numunelerin nihai özelliklerini doğrudan etkilemiştir. Ube ve SicoNide tozu için sinterlenmiş yoğunluklar 3 saat sonunda sırasıyla 3.04 ve 2.86 g/cm^3 olarak elde edilmiştir. XRD analizi SicoNide tozunun ağırlıkça % 10 civarında β-Si_3N_4 içerdiğini göstermiştir. FTIR çalışması da bu fazın varlığını desteklemektedir. β fazının α'ya kıyasla daha düşük reaktiviteye sahip olması nedeniyle yoğunlaşma gecikmiştir. Ana faz β-Si_3N_4, α-Si_3N_4 ve Si_2N_2O ise ikincil fazlar olarak oluşmuştur. Üç saat sinterlenen numunelere yapılan SEM analizinde büyük β taneleri gözlemlenmiştir. Sertlik, kırılma tokluğu ve dielektrik sabiti değerleri sırasıyla 12.5 GPa, , 5.8 MPa.m$^{-1/2}$ and 7.84 olarak ölçülmüştür. Bu sonuçlar düşük maliyetli Si_3N_4 üretimi için havada sinterlemenin uygun bir alternatif olabileceğini göstermiştir.

Anahtar Kelimeler: *Si_3N_4, Havada sinterleme; Başlangıç tozu; Sinterleme süresi; Yoğunlaşma.*

1. Introduction

Several difficulties have been encountered during the sintering of dense Si_3N_4 ceramics; the necessity for a protective atmosphere, the demand of high temperature-pressure values, and the risk of decomposition into Si (l,g) and N_2 (g) at elevated temperatures. Therefore, sintering is performed in specific furnaces that operate at high temperature-pressure and provide N_2 or other protective atmospheres. This limits the widespread production and application of Si_3N_4 ceramics. One solution to overcome this problem is performing air sintering. However, the presence of O_2 in the air is very detrimental at high temperatures for Si_3N_4 ceramics (Luo et al. 2021, Wada 2001, Wada et al. 2004, Zhao et al. 2019). If the partial pressure of oxygen is high, passive oxidation takes place. In the case of lowering the pressure, the oxidation process is changed to an active one. This change from passive to active occurs around 10^2 Pa (Wangmooklang et al. 2007). In passive oxidation, a protective layer has been formed with nm thickness whose composed of SiO_2 or Si_2N_2O. Volatile suboxide has been produced during active oxidation (Long et al. 2017). Mass reduction and delamination of the surface layer could be examined.

Some researchers investigate the feasibility of sintering Si_3N_4 ceramics under air conditions at moderate temperatures. Wada et al. (2001) proposed using a basic double crucible setup to completely isolate Si_3N_4 from air. Al_2O_3 had been preferred as the crucible material owing to its inert, antioxidant nature and resistance against high temperatures. During double crucible sintering, Si_3N_4 can react with O_2 from two sources; O_2 from the Al_2O_3 crucible and O_2 from the gap between the crucible and lid. Therefore, crucibles must be filled with powder bed to avoid reaction with O_2. A tight-fitting lid also could be used to ensure the isolation of Si_3N_4 from O_2 presence. Stability is another problem that must be overcome

*Sorumlu Yazar/Corresponding Author: Adı Soyadı e-posta/e-mail: yazaradı@aku.edu.tr

during the sintering. Dense Si_3N_4 is generally sintered higher than 1650°C and atmospheric pressure. According to the stability diagram of Si3N4, the sinterability region diminishes as temperature increases and it tends to decompose. This can be suppressed by increasing N_2 pressure (Wada 2001). Since air sintering is done under atmospheric conditions, lower sintering temperatures must be selected. This may limit the consolidation of ceramic and therefore a high amount of sintering agents up to 15 wt. % has been used in air sintering studies. The other critical parameter is the type of sintering agent. To decrease the densification temperature, agents providing lower eutectics must be chosen. By using alkali and alkaline-earth oxides, a low melting point and a liquid phase with low viscosity can be achieved which are advantageous for densification. However, the risk of instability and evaporation of these agents must be taken into account (Matovic 2003). Matovic (2003) concluded that the sintering temperature can be decreased to 1500°C from 1900°C by using various amounts of Al_2O_3 and Y_2O_3. Osahi et al. (1991) showed that the Al_2O_3-SiO_2-Si_3N_4 system has a eutectic point at 1470°C. The eutectic temperature of the binary Y_2O_3-SiO_2 system is 1660°C, the addition of Si_3N_4 lowers the temperature to 1550°C (Plucknett et al, 2008). Therefore, Al_2O_3 and Y_2O_3 are the most common sintering agents preferred in air sintering studies.

Besides initial powder and sintering agents, parameters like size and type of packing powder, using open or closed crucible, and sintering temperature/duration have been studied in air sintering studies (Wada 2001, Wada *et al*. 2001, Wada *et al*. 2004, Plucknet and Lin 2005).

This study aims to sinter Si_3N_4 ceramics in an air atmosphere at a moderate temperature. Two different Si_3N_4 powders have been used to investigate the effect of starting powder type on the final properties. The density and mechanical and dielectric properties of produced samples are very promising for low-cost and widespread fabrication of high-quality Si_3N_4 ceramics.

2. Materials and Methods

Two types of Si_3N_4 powders were used to observe the effect of Si_3N_4 source on the final properties. Ube E-10 (Ube Industries, specific surface area 9-13 m^2/g, < 2.0 wt. % O, > 95 wt. % α-Si_3N_4) and Siconide P95H (Vesta Si Ceramics, specific surface area 10-12 m^2/g, < 1.5 wt. % O_2, >91 wt. % α-Si_3N_4) were selected. Fourier transform infrared spectroscopy (FTIR) analysis (Perkin Elmer, Spectrum 100) of both powders was done to identify functional groups. 90 wt. % of Si_3N_4 source was mixed with 8 wt. % of Al_2O_3 (Honeywell, Fluka) and 2 wt. % of Y_2O_3 (Grade C, H.C. Starck) with a ball mill at 180 rpm for 24 h in isopropyl alcohol. Compositions are given in Table 1. The rotary evaporation process was used to obtain finely dispersed powders. Samples were compacted by using a uniaxial dry pressing (MSE Technology) under 100 MPa pressure. Samples were completely isolated by using a double crucible setup (Figure 1.) during sintering. They are put into an inner crucible filled with Si_3N_4 powder whose content is identical to the samples. Since the presence of oxygen is critical for passive oxidation, Al_2O_3 powder was used as the second powder bed. Sintering was done in an air atmosphere furnace with $MoSi_2$ heating element (MSE Technology) at 1550°C for 1 and 3 h.

Table 1. Compositions used in this study

Composition	Si_3N_4 powder type	Si_3N_4 (wt. %)	Al_2O_3 (wt. %)	Y_2O_3 (wt. %)
U	Ube E-10	90	8	2
S	SicoNide P95H	90	8	2

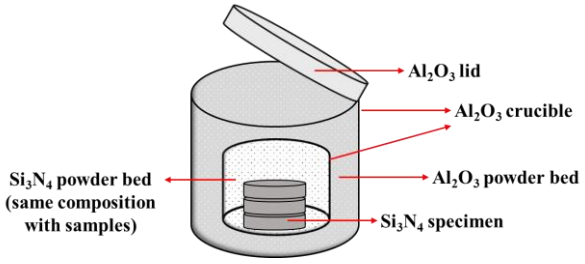

Figure 1. Schematic description of double crucible setup

Archimedes' displacement method was used for density measurement (Elsen and Ramesh, 2016). X-ray diffraction (XRD) (Rigaku MiniFlex–600, Japan) analysis was done for both powders and all samples. The weight ratio of β-Si_3N_4 was calculated by Equation 1. (Pigeon and Varma, 1992). Intensities of (101) and (210) planes from β-Si_3N_4, and (102) and (210) planes from α-Si_3N_4 were used as seen in Eq. 1.

$$\beta\text{–}Si_3N_4 = \frac{\beta(101)+\beta(210)}{\beta(101)+\beta(210)+\alpha(102)+\alpha(210)} \times 100 \quad (1)$$

A scanning electron microscope (SEM) (Zeiss Supra 40 VP, Germany) was used to observe the microstructural development of samples. The dielectric constant was measured using an inductance–capacitance–resistance meter (Agilent 4294A) at 5 MHz. The hardness and fracture toughness were measured by the indentation method (Shimadzu HMV-G, Japan) with a 10 N load for ten seconds from the polished surface of the samples.

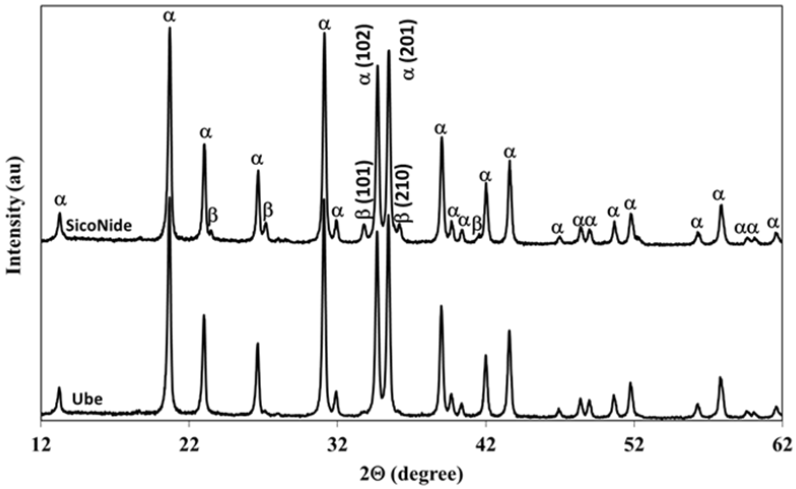

Figure 2. XRD patterns of initial Si_3N_4 powders

3. Results and Discussion

XRD patterns of initial Si_3N_4 powders can be seen in Figure 2. The major phase of both powders was identified as α-Si_3N_4 while the presence of β-Si_3N_4 was detected in SicoNide powder. The amount of β phase was found as 10.73 % according to Eq. 1. Negligible amount of β is present in Ube powder.

The IR spectra of the initial Si_3N_4 powders are given in Figure 3. For both powders, frequency variations are small, frequency and intensity of IR bands are nearly the same. The main differences are; a) intensity of broad band between 750-850 cm^{-1}, b) formation of new peak at 576 cm^{-1} for SicoNide and c) peak intensity around 480 cm^{-1}.

Amorphous Si_3N_4 has an intense broad band centered at 840 cm^{-1}, for Ube powder, this band is greater (Trout *et al.* 1989).

Mazdiyasni and Cooke (1973) produced Si_3N_4 powder by thermal decomposition of $Si(NH)_2$ between 1000-1500°C and examined the powder by IR spectroscopy. They concluded that as the decomposition temperature was increased, IR peaks shifted to lower frequencies, and additional peaks at near 570 and 440 cm^{-1} were found as a result of β-Si_3N_4 formation. Skoop et al. (1990) proved the presence of β phase for the lines at 400 and 575 cm^{-1}. Therefore, the band observed at 576 cm^{-1} in SicoNide proved the presence of β-phase. Also, this result is consistent with the XRD pattern of SicoNide where β phase appeared. Si–N symmetric stretching mode at 480 cm^{-1} is higher for SicoNide. Signals around 458, 510, 599, 675 and 685 cm^{-1} belong to vibrations in α-Si_3N_4. The IR peaks between 800-1050 belong to antisymmetrical Si-N stretching greater (Trout *et al.* 1989).

Table 2. shows properties related to densification. Weight loss values measured were less than 1% that are consistent with previous studies (Wada 2001, Wada et al. 2001, Plucknett 2009). Values proved the prevention of oxidation where high weight gains are observed in both passive and active forms. Higher shrinkage values were achieved with high bulk density and low apparent porosity.

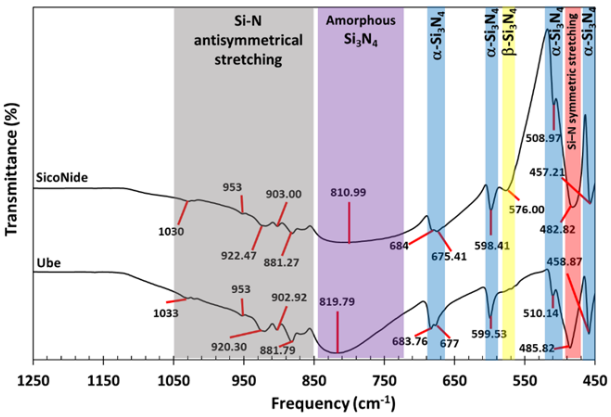

Figure 3. IR spectra of initial Si_3N_4 powders

Wada et al. (2004) showed a lag between furnace and crucible temperatures at the early stage of sintering and concluded that the crucible reached the furnace temperature after 3 h. Therefore, denser samples were produced from U3 and S3. The apparent porosity reached to 0.37% for sample U3. Although S samples have higher green density, the final bulk densities of these samples were lower for both temperatures. The main reason was the amount of β phase present in SicoNide powder.

Densification of Si_3N_4 occurs by a liquid-phase sintering into three stages; rearrangement, solution–precipitation and microstructure coarsening Sintering agents react with the oxygen layer that exists on the surface of each Si_3N_4 particle and form a liquid phase, which is responsible for the rearrangement process. Si_3N_4 particles dissolve in this liquid, and as it reaches the supersaturation, β phase

precipitates which is responsible for densification. Compare to α-Si_3N_4, β phase has fewer defects, less oxygen content and higher stability which retard dissolution, hence densification was delayed for S samples (Xie *et al*. 2019 Peng 2004, Björklund *et al*. 1997). U3 has the lowest apparent porosity among all samples, but its bulk density is still smaller than that of the theoretical density of Si_3N_4 (3.19 g/cm^3).

XRD patterns of samples are given in Figure 4. For U1, the major phase was α-Si_3N_4, Si_2N_2O, and β-Si_3N_4 were detected as the other phases. As the sintering time increased to 3 h, β-Si_3N_4 had the highest intensity with a small amount of Si_2N_2O and α-Si_3N_4. Since crucible and furnace temperatures became equal at 3 h, a larger volume of liquid phase was present that enhanced the development of β-Si_3N_4. Also, the higher content of sintering additives affected α to β transformation.

Table 2. Density characteristics of samples

Sample	Green density (g/cm^3)	Weight Loss (%)	Linear Shrinkage (%)	Bulk Density (g/cm^3)	Apparent Porosity (%)
Ube-1550-1 (U1)	1.46	0.56 (±0.05)	22.09 (±0.61)	2.97 (±0.01)	2.40 (±0.16)
Ube-1550-3 (U3)		0.94 (±0.04)	22.58 (±0.08)	3.04 (±0.03)	0.37 (±0.22)
Siconide-1550-1 (S1)	1.50	0.37 (±0.14)	19.39 (±0.36)	2.78 (±0.03)	3.57 (±0.95)
Siconide-1550-3 (S3)		0.81 (±0.23)	20.48 (±0.14)	2.86 (±0.02)	1.44 (±0.14)

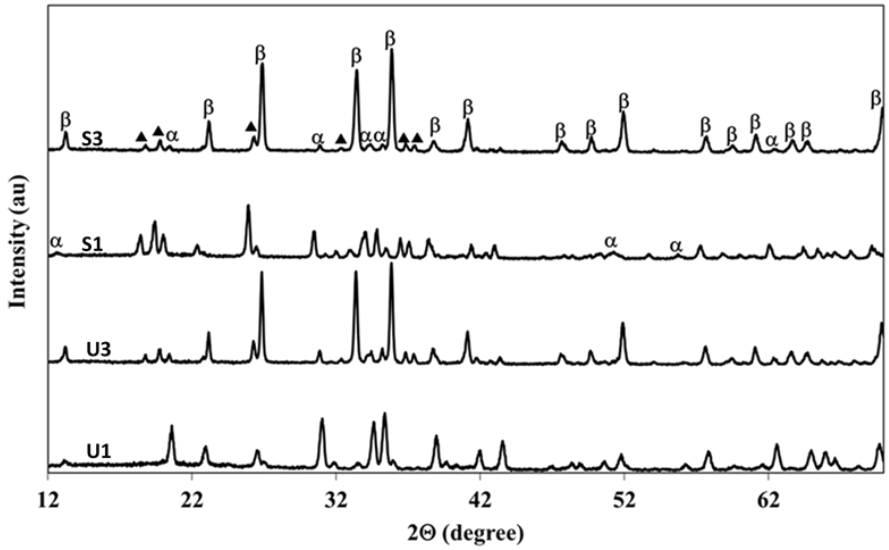

Figure 4. XRD patterns of Si_3N_4 samples (α: α-Si_3N_4, β:β-Si_3N_4 and ▲:Si_2N_2O

A higher percentage of sintering aids in Si_3N_4 ceramics is favorable for polymorphic transformation since α-Si_3N_4 dissolves more readily in the liquid phase and transforms to β-Si_3N_4 through the dissolution–precipitation reaction. (Kim et al. 2022) Si_2N_2O was the major phase with a considerable amount of α and β-Si_3N_4 for S1. S3 has the same behavior as U3, the major phase formed was β-Si_3N_4 with Si_2N_2O and α-Si_3N_4. Lower bulk density values for U3 and S3 samples can be explained by the presence of Si_2N_2O. Since the density of this phase is 2.82-2.85 g/cm^3, it reduced the bulk densities even with low apparent porosity values (Sekercioglu and Willis 1979, Wada *et al.* 2001).

The calculated β wt. % is given in Table 3. Due to the presence of β phase in SicoNide powder, samples S have higher β ratios. Around a 5-fold increase in β content was obtained for sample U3 as the sintering temperature was raised to 3 h. The rise was just 3.5-fold for sample S3. The sluggish reactivity of β-Si_3N_4 also resulted in a lower increase in β ratios as well as lower densities.

Table 3. Calculated β-Si_3N_4 ratios (wt. %)

Sample	β-Si_3N_4 ratio (wt. %)
U1	16.78
U3	86.28
S1	25.46
S3	90.04

SEM-SE images of samples are given in Figure 5 (a-d). A higher amount of residual porosity was apparent both in U1 and S1 compared to U3 and S3. Grain morphology is quite different in S1 compared to U1, microstructure consisting of fine, equiaxed grains in U1 (Figure 5a), coarse, sharp-edged, anisotropic grains (indicated by yellow arrows) are present which can be attributed to Si_2N_2O in S1 (Figure 5b).

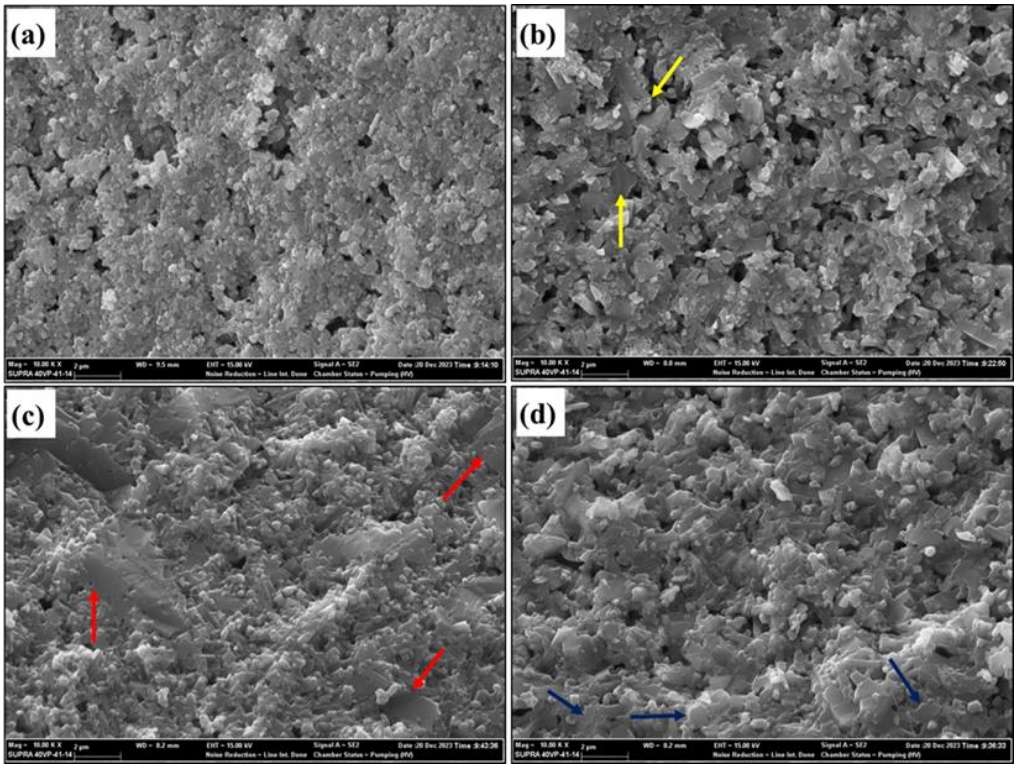

Figure 5. SEM-SE images of (a) U1, (b) S1, (c) U3 and (d) S3

The same morphology was concluded for Si_2N_2O in previous studies (Wada et al. 2004, Plucknett and Lin). At higher sintering times, the amount of liquid phase rose and enhanced consolidation. An obvious reduction in porosity was observed from both samples sintered at 3 h. Coarser and highly anisotropic β grains (indicated by the red arrow) are present in U3 with negligible residual porosity. Same grain morphology was obtained by Plucknett and Lin (2006) at 1600°C, Plucknett (2009) at 1700°C, Wada et al. (2004) and Wangmooklang et al. (2007) at 1700°C whose temperatures are relatively higher compared to this study. The sintering time was selected as 2 h for all studies and lower sintering time may result in insufficient densification.

The dielectric and mechanical properties of samples are given in Table 4. Dielectric constant values were between 6.84 to 7.84 which are compatible with density values. The highest constant was obtained for U3 whose density was also the highest. There is a large variation in dielectric constant values of Si_3N_4 according to the previous studies depending on the secondary phases, porosity and measurement frequency. Barta *et al*. (1985) measured the dielectric constant of dense Si_3N_4 as 8.5 at MHz range, Dai *et al*. (2021) found the value as 11 at 12.4 GHz. The same frequency was used by Lee and Baek (2016) and depending on the porosity content, constant reduced from 7.66 (porosity was 3.7%) to 4.76 (porosity was 24.5%) Porosity also affected the hardness of samples. Higher hardness values reached for U3 and S3 samples were 12.5 and 12.8, respectively. Wangmooklang *et al.* (2007) measured the hardness as 12.07 and 13.4 GPa from the samples sintered at 1700°C in air and N_2, respectively. A significant effect of microstructure on fracture toughness was observed between U1 and U3. As the amount of β-Si_3N_4 increased, values improved from 4.4 and to 5.8 MPa.m$^{-1/2}$. Since the polished surfaces of sample S are not suitable, toughness values were not measured. The same authors obtained the fracture toughness values 5.5 and 6 MPa.m$^{-1/2}$ for air and N_2 atmospheres (Wangmooklang *et al.* 2007). The result is very promising since nearly the same hardness value was achieved nearly 150°C lower for this study.

Table 4. Dielectric constant and mechanical properties of samples

Sample	Dielectric Constant @ 5 MHz	Hardness (GPa)	Fracture Toughness (MPa.m$^{-1/2}$)
U-1	7.48	11.3 (±0.9)	4.4 (±0.3)
U-3	7.84	12.5 (±0.1)	5.8 (±0.2)
S-1	6.84	11.6 (±0.6)	Not measured
S-3	7.39	12.8 (±0.7)	Not measured

When the obtained mechanical properties are compared with the studies where high temperature and controlled atmosphere were used, significant differences were

observed. The hardness values of Si_3N_4 sintered at 1750°C for 1 h under 6 MPa N_2 pressure measured as 16.75 and 16.50 GPa when 5 wt. % Yb_2O_3-2wt.% Al_2O_3 and 5 wt. % CeO_2-2wt.% Al_2O_3 were used, respectively. The fracture toughness was 8.9 and 9.5 MPa.$m^{-1/2}$ for the same samples (Yang et al, 2019). Du et al. produced Si_3N_4 from powders mixtures where the weight ratio of Si_3N_4: MgO: RE_2O_3 is 90:2:8 with a sintering process at 1800°C and under a N_2 pressure of 3 MPa for 8 h. The highest hardness value was almost 13 GPa from Nd_2O_3 doped sample, the highest fracture toughness was achieved as 7.75 MPa.$m^{-1/2}$ where Gd_2O_3 was used as rare earth additives (Du *et al.* 2024).

Although the mechanical properties of air-sintered Si_3N_4 are relatively lower compared to high temperature and N_2 pressure sintered counterparts, these Si_3N_4 ceramics can be a good candidate for applications where moderate mechanical resistance is expected. Considering the dielectric constant, air-sintered Si_3N_4 can be a substrate material in electronic circuits and diveces. The other promising application can be bioceramics. Moderate mechanical properties may minimize stress shielding by reducing the difference of mechanical properties between bone and Si_3N_4 implant.

4. Conclusions

Air sintering provides an economically feasible and straightforward process for the production of Si3N4 ceramics. Substantially lower porosity and higher density were achieved under atmospheric pressure and moderate sintering temperature (1550°C) by using a double crucible setup. Sintering time and type of Si_3N_4 powder influenced the final properties. As time increased to 3 h, densification improved via transformation from α to β-Si_3N_4 phase. The lowest apparent porosity value reached was 0.37%. Also, hardness and fracture toughness values were very close to samples that are sintered at higher temperatures and N_2 atmosphere. The presence of β-phase in SicoNide powder retards densification and lowers the density values of the samples.

Declaration of Ethical Standards

The author declares that she complies with all ethical standards.

Credit Authorship Contribution Statement

Author 1- Conceptualization, Methodology/Study design, Investigation, Writing-original draft.

Declaration of Competing Interest

The author declares that she has no known competing financial interests or personal relationships that could have appeared to influence the work reported in this paper.

Data Availability Statement

The author declares that the main data supporting the findings of this work are available within the article.

5. References

Barta, J., Manela, M. and Fischer, R., 1985. Si_3N_4 and Si_2N_2O for high performance radomes. *Materials Science and Engineering,* **71**, 265-272. https://doi.org/10.1016/0025-5416(85)90236-8

Björklund, H., Falk, L. K. L., Rundgren, K., and Wasén, J. 1997. β-Si_3N_4 grain growth, part I: Effect of metal oxide sintering additives. *Journal of the European Ceramic Society*, **17(11)**, 1285-1299. https://doi.org/10.1016/S0955-2219(96)00237-3

Dai, Q., He, D., Meng, F., Liu, P. and Liu, X., 2021. Dielectric constant, dielectric loss and thermal conductivity of Si_3N_4 ceramics by hot pressing with CeO_2–MgO as sintering aid. *Materials science in semiconductor processing*, **121**, 105409. https://doi.org/10.1016/j.mssp.2020.105409

Du, S., Li, F., Zhang, J., Chen, Z., Zhang, S., Zhao, S., Zhao D., Fan, B., Chen, K. and Liu, G. 2024. Effects of sintering additives and sintering methods on the mechanical, antimicrobial and optical properties of Si_3N_4 bioceramics. *Journal of the Mechanical Behavior of Biomedical Materials*, **154**, 106529. https://doi.org/10.1016/j.jmbbm.2024.106529

Elsen, S. R., and Ramesh, T., 2016. Analysis and optimization of dry sliding wear characteristics of zirconia reinforced alumina composites formed by conventional sintering using response surface method. *International Journal of Refractory Metals and Hard Materials*, **58**, 92-103.

https://doi.org/10.1016/j.ijrmhm.2016.04.007

Kim, K. A., Lysenkov, A. S., Fedorov, S. V., Petrakova, N. V., Frolova, M. G., Perevislov, S. N. and Kargin, Y. F., 2022. Effect of CaO–Al_2O_3 (48: 52 wt%) Sintering Aids on the Phase Composition and Properties of Si_3N_4-Based Ceramics. *Inorganic Materials*, **58 (8)**, 877-885. https://doi.org/10.1134/S0020168522080040

Lee, S. J. and Baek, S., 2016. Effect of SiO_2 content on the microstructure, mechanical and dielectric properties of Si_3N_4 ceramics. *Ceramics International*, **42 (8)**, 9921-9925. https://doi.org/10.1016/j.ceramint.2016.03.092

Long, M., Li, Y., Qin, H., Xue, W., Jiang, P., Sun, J. and Kumar, R. V., 2017. Mechanism of active and passive oxidation of reaction-bonded Si_3N_4-SiC refractories. *Ceramics International*, **43 (14)**, 10720-10725. https://doi.org/10.1016/j.ceramint.2017.05.044

Luo, C., Zhang, Y.,and Deng, T., 2021. Pressureless sintering of high performance silicon nitride ceramics at 1620 °C. *Ceramics International*, **47 (20)**, 29371-29378.

https://doi.org/10.1016/j.ceramint.2021.07.104

Matovic, B., 2003. Low Temperature Sintering Additives for Silicon Nitride. Ph.D. Dissertation, Stuttgart University, Institute of Non-metallic Anorganic Materials, Stuttgart, 34.

Mazdiyasni, K. S. and Cooke, C. M., 1973. Synthesis, characterization, and consolidation of Si_3N_4 obtained from ammonolysis of $SiCl_4$. *Journal of the American Ceramic Society*, **56** (12), 628-633 https://doi.org/10.1111/j.1151-2916.1973.tb12440.x

Ohashi, M., Kanzaki, S., and Tabata, H. 1991. Effect of additives on some properties of silicon oxynitride ceramics. *Journal of materials science*, **26**, 2608-2614. https://doi.org/10.1007/BF00545544

Peng, H. 2004. Spark Plasma Sintering of Si_3N_4-Based Ceramics: Sintering mechanism-Tailoring microstructure-Evaluating properties, Ph.D. Dissertation, Stockholm University, Department of Inorganic Chemistry, 8-17.

Pigeon, R. G., and Varma, A. 1992. Quantitative phase Analysis of Si_3N_4 by X-ray diffraction. *Journal of materials science letters*, **11**, 1370-1372. https://doi.org/10.1007/BF00729365

Plucknett, K., 2009. Sintering Behavior and Microstructure Development of Porous Silicon Nitride Ceramics Prepared in an Air Atmosphere Furnace. *International Journal of Applied Ceramic Technology*, **6** (6), 702-716. https://doi.org/10.1111/j.1744-7402.2008.02309.x

Plucknett, K. P. and Lin, H. T., 2005. Sintering silicon nitride ceramics in air. *Journal of the American Ceramic Society*, **88** (12), 3538-3541. https://doi.org/10.1111/j.1551-2916.2005.00631.x

Sekercioglu, I. and Wills, R. R., 1979. Effect of Si_3N_4 Powder Reactivity on the Preparation of the Si_2N_2O-Al_2O_3 Silicon Aluminum Oxynitride Solid Solution. *Journal of the American Ceramic Society*, **62** (11-12), 590-593. https://doi.org/10.1111/j.1151-2916.1979.tb12738.x

Trout, T. K., Bellama, J. M., Brinckman, F. E. and Faltynek, R. A., 1989. Fourier transform infrared analysis of ceramic powders: Quantitative determination of alpha, beta, and amorphous phases of silicon nitride. *Journal of Materials Research*, **4** (2), 399-403. https://doi.org/10.1557/JMR.1989.0399

Wada, S. (2001). Control of instability of Si_3N_4 during pressureless sintering. *Journal of the Ceramic Society of Japan*, **109** (1274), 803-808. https://doi.org/10.2109/jcersj.109.1274_803

Wada S., Chaiyapak, P., Jinawath, S. and Wasanapiarnpong, T., 2004. Sintering of Si_3N_4 ceramics in air atmosphere furnace (Part 2)-Agglomeration of packing powder and deterioration of Al_2O_3 crucible. *Journal of the Ceramic Society of Japan,* **112** (1304), 234-237. https://doi.org/10.2109/jcersj.112.234

Wada S. Hattori T. and Yokoyama K., 2001. Sintering of Si_3N_4 ceramics in air atmosphere furnace, *Journal of the Ceramic Society of Japan,* **100** *(3) 281-283.* https://doi.org/10.2109/jcersj.109.1267_281

Wangmooklang, N., Sujirote, K., Jinawath, S. and Wada, S. 2007. Gas/solid reaction during sintering of Si3N4 ceramics in an air furnace. *Journal of the European Ceramic Society*, **27** (4), 2111-2117. https://doi.org/10.1016/j.jeurceramsoc.2006.06.004

Xie, L., Yao, D., Xia, Y., Yin, J., Liang, H., Zuo, K., and Zeng, Y. 2019. High porosity Ca-α-SiAlON ceramics with rod-like grains fabricated by freeze casting and pressureless sintering. *Journal of the European Ceramic Society*, **39(6)**,2036-2041. https://doi.org/10.1016/j.jeurceramsoc.2019.01.027

Yang, L., Ditta, A., Feng, B., Zhang, Y., and Xie, Z. 2019. Study of the comparative effect of sintering methods and ,sintering additives on the microstructure and performance of Si_3N_4 ceramic. *Materials*, ***12*****(13)**, 2142. https://doi.org/10.3390/ma12132142

Zhao, S., Wang, Z., Li, L., Guo, A., Wang, G. and Li, H., 2019. Sintering Behavior of Si_3N_4 Ceramics at Low Temperature in Air Atmosphere Furnace. *IOP Conference Series, Materials Science and Engineering*, Kunming, China, 012045.